Solvent-Induced Structural Changes in Complexes of 1,2-Bis(3-(3-pyridyl)pyrazolyl)ethane

Yuniar P. Prananto,[A] *David R. Turner,*[A] *Jinzhen Lu,*[A] *and Stuart R. Batten*[A,B]

[A]School of Chemistry, Monash University, Clayton, Vic. 3800, Australia.
[B]Corresponding author. Email: stuart.batten@sci.monash.edu.au

A series of complexes have been obtained using the flexible ditopic ligand 1,2-bis(3-(3-pyridyl)pyrazolyl)ethane (L^{Et}) with $M(SCN)_2$ (M = Co, Fe) and $ZnCl_2$. The ligand is observed to exist in a variety of conformations with rotations around the ethane spacer and around the pyridyl/pyrazole bond. The bridging length of the ligand (i.e., distance between pyridyl nitrogen atoms) varies by 3.5 Å depending on its geometry. Three different cobalt(II) complexes of the general form $[Co(L^{Et})_2(SCN)_2]\cdot$Solv (where Solv is a variable number/type of non-coordinated solvent) have been structurally characterized and form a series of solvent dependant supramolecular isomers. When Solv = 2MeCN a (4,4)-sheet is formed (**1**), however, when Solv = H_2O an alternate 'collapsed' (4,4)-sheet is observed (**2**). Changing the solvent to two molecules of *N,N*-dimethylformamide (DMF) leads to a radical change in structure with a one-dimensional (1D) polymer formed (**3**) that contains two bridging ligands between adjacent metal atoms (i.e., maintaining the same metal/ligand ratio as in the (4,4)-sheet structures). A monomeric thiocyanate complex $[Fe(L^{Et})_2(SCN)_2(H_2O)_2]$ (**4**) is reported in which the bispyridyl ligands are terminal and partake in an extended hydrogen-bonded network. A 1D polymer $[Zn(L^{Et})Cl_2]$ (**5**) is also presented. The structures of the metal complexes are contrasted with that of the free ligand.

Introduction

The synthesis of coordination polymers through self-assembly, by definition, removes a significant amount of control from the experimental chemist.[1–3] A judicious choice of ligands and the selection of metal ions with a propensity towards desired coordination geometries allows one to predict the product to a certain extent, however, there is no guarantee that even the most well designed system will actually form when the reagents are left to their own devices. In the main, self-assembly is a thermodynamically controlled process with the most stable product forming under the specific conditions that are used.[4] Subtle changes in the reaction conditions, e.g., temperature, pressure, or solvents, can yield vastly different products as is often displayed in the synthesis of aluminosilicate networks (i.e., zeolites). The synthesis of coordination polymers under self-assembling conditions frequently yields surprising results and this unpredictability leads to a plethora of exciting networks.[5]

Introducing flexibilty into bridging ligands can introduce an extra element of uncertainty into the formation of coordination polymers and raise the possibility of interpenetration and/or polymorphism.[6] While ligands such as 4,4′-bipyridine act as very rigid linear connectors, dipyridyl ligands with spacer groups such as $(CH_2)_x$ or aryl linkers can produce a wide variety of bridging geometries (while remaining topologically linear).[7] There are numerous examples of coordination polymers that contain flexible bridging ligands that in turn contain heterocyclic N-donor groups such as imidazole,[8] triazole,[9] and tetrazole.[10] The flexibility in these ligands also allows for the fomation of metallomacrocycles in some instances when combined with appropriate, *cis*-coordinating metals (i.e., $Pd(dppp)_2^+$, where dppp = 1,3-bis(diphenylphosphino)propane).[11]

Herein we report the synthesis of a novel, flexible bridging ligand, 1,2-bis(3-(3-pyridyl)pyrazol-1-yl)ethane (L^{Et}), and the syntheses and structures of several complexes with transition metals. The ligand is able to form both one- (1D) and two-dimensional (2D) polymeric complexes with $Co(SCN)_2$, depending on the solvent used, and is observed in a monodentate binding mode within a discrete mononuclear species. In addition we have observed a 1D polymer when the ligand is combined with $ZnCl_2$. The ligand displays a remarkable variety of geometries with the distance between the terminal pyridyl nitrogen atoms varying between 11.22 and 14.77 Å.

Results and Discussion

Synthesis and Structure of L^{Et}

The bispyrazolyl ligand L^{Et} was synthesized by the reaction of 3-(3-pyridyl)pyrazole[12] with 1,2-dibromoethane in the presence of base (Scheme 1). The product is obtained in good yield and is easily purified. This reaction is in contrast to that attempted using 2,6-dibromopyridine as a spacer between pyrazolyl groups (in place of the current ethane spacer) whereby only a single bromine is displaced and the desired ligand is not obtained.[13] It should be noted that the substitution of the pyrazole group in the 3-position (relative to the NH) is the only isomer formed (i.e., there is no product that contains the pyridyl group in the 5-position). Ditopic ligands that contain pyrazolyl/pyridyl arms have been shown to be able to form extended networks, although all previous reports of such species are 4-pyridyl derivatives.[14] Flexible ligands that contain 2-pyridyl have also been explored, although these tend to result in molecular species.[15]

Crystals of the ligand were obtained by diffusion of diethylether into a methanolic solution of L^{Et}. The crystals grow
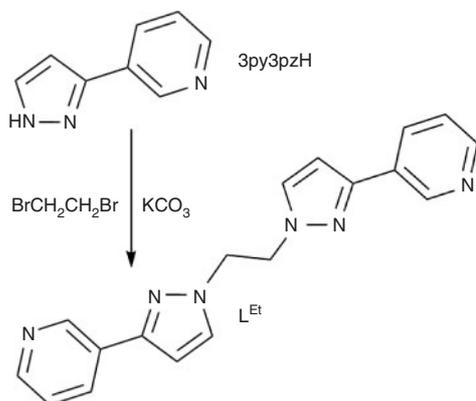
**Scheme 1.** Synthesis of the ethane bridged bispyrazolyl ligand L^{Et}.
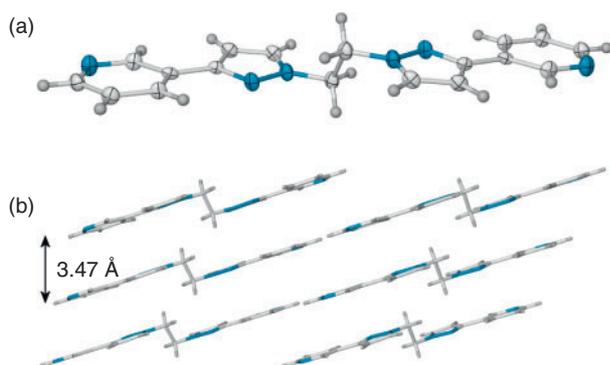
Fig. 1. (a) The molecular structure of the L^{Et} species in a *trans*-geometry (ellipsoids displayed at 50% probability) and (b) crystal packing, dominated by face-to-face π-interactions.

in the space group $P2_1/c$ and contain one-half of the molecule in the asymmetric unit (i.e., there is an inversion centre midway along the ethane bridge). The molecule adopts a *trans* geometry with the arms on opposite sides of the ethane bridge. The pyridyl/pyrazolyl rings within the 'arms' of the ligand are slightly removed from being co-planar (by 4.5°), however, the mean planes of the two arms are parallel (enforced by the crystallographic symmetry). The pyridyl nitrogen atom is facing towards the opposite side of the molecule to the pyrazolyl nitrogen atoms. Packing in the structure is dominated by face-to-face interactions between the π-systems of adjacent molecules. Stacks of L^{Et} molecules are aligned parallel to the *a*-axis with a separation of 3.47 Å between the mean planes of neighbouring pyridyl/pyrazolyl arms. There are no acidic protons to form strong hydrogen bonds, however, there are weak CH···N interactions that involve the pyridyl nitrogen atom with a CH_2 proton and a pyrazolyl proton (H···N = 2.49 and 2.63 Å, respectively). There are other, longer CH···N contacts that involve a CH_2···pyridyl contact (2.85 Å) and both Hpy···Npz and Hpz···Npz interactions to the non-substituted pyrazole nitrogen atom (2.79 and 3.00 Å, respectively).

Supramolecular Isomers of L^{Et} with Co(SCN)$_2$

Three complexes were obtained by the reaction of L^{Et} with Co(ClO$_4$)$_2$ and Na(SCN) in various solvents, namely [Co(L^{Et})$_2$(SCN)$_2$]·2MeCN (**1**), [Co(L^{Et})$_2$(SCN)$_2$]·2H$_2$O (**2**),
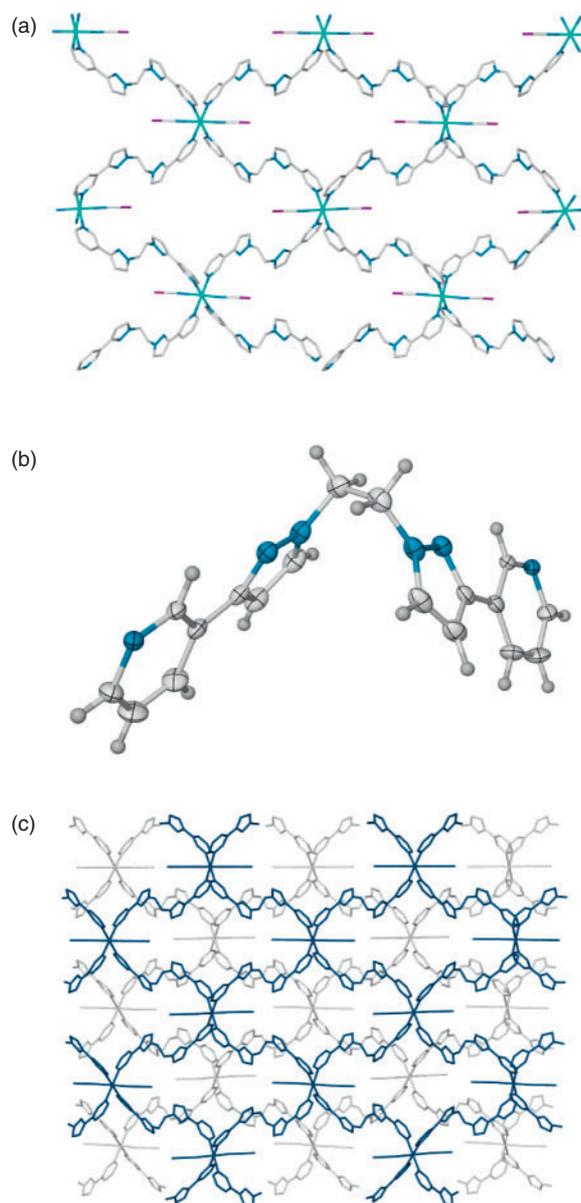
Fig. 2. (a) The (4,4) sheet structure formed in the complex [Co(L^{Et})$_2$(SCN)$_2$]·2MeCN (**1**) (hydrogen atoms and solvent molecules are omitted for clarity). (b) The *cis*-geometry of the L^{Et} ligand (ellipsoids displayed at 50% probability, cf. Fig. 1a). (c) The sheets pack in an offset manner (only two sheets shown for clarity).

and [Co(L^{Et})$_2$(SCN)$_2$]·2DMF (**3**) (DMF = *N,N*-dimethylformamide) (see experimental data). These three complexes contain the same metal/ligand/anion ratio and differ only in the lattice solvent, however, the structures of these products are significantly different from each other. The products, **1**–**3**, are supramolecular isomers as, although compositionally similar, the structures differ depending upon the solvent that is present.[16]

The compound [Co(L^{Et})$_2$(SCN)$_2$]·2MeCN (**1**) crystallizes in the orthorhombic space group *Cmca* (see experimental section). The asymmetric unit contains half of the metal atom, half of an L^{Et} ligand, one SCN ligand, and a lattice acetonitrile molecule. The polymeric complex forms a (4,4) sheet in which the Co atoms act as the four-connecting nodes and the L^{Et} ligands can be considered as linear bridging ligands (Fig. 2a). The holes in the (4,4) sheet have dimensions of 17.0×23.4 Å^2 (measuring

(a)

(b)
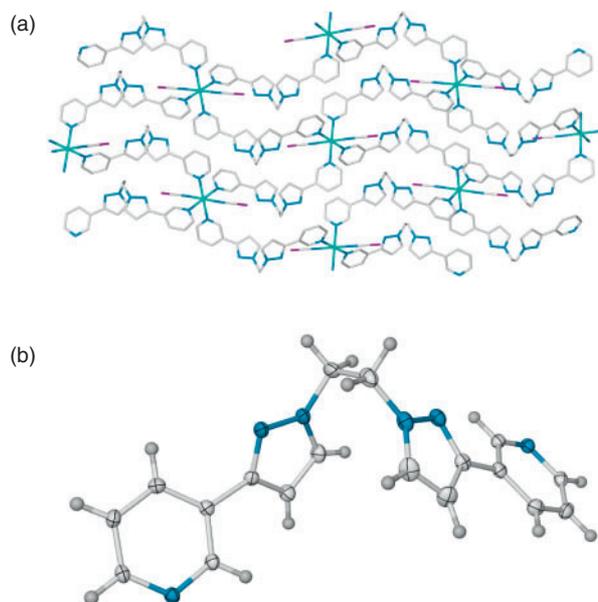
Fig. 3. (a) The (4,4) sheet formed in the structure of [Co(L^{Et})$_2$(SCN)$_2$]·2H$_2$O (**2**) is very different from that observed in the acetonitrile solvate (**1**, see Fig. 2). (b) The geometry of the ligand is different from that in **1** because of a change in the relative orientations of the pyridyl and pyrazolyl rings.

between Co atoms). The ligands in the structure of **1** adopt a radically different geometry compared with those observed in the crystal structure of the free ligand (see above) with the arms of the bridging ligand arranged in a *cis*-geometry around the central ethane bridge (Fig. 2b). The arms are also less planar than they are in the free ligand with the angle between the pyridyl and pyrazolyl ring being 12.0°. In another change from the structure of L^{Et}, the pyridyl nitrogen atoms in the ligand in **1** are on the same side of the ligand as the pyrazolyl nitrogen atoms. The packing of the sheets is arranged such that the metal atom resides over the centre of the hole in the adjacent sheets (Fig. 2c). The mean planes of the arms in adjacent sheets are separated by 3.11 Å and are offset from each other with the shortest H$_{py}$···pyridyl ring centroid distances being 3.64 and 3.46 Å. The acetonitrile molecules are held in the lattice by two CH···N≡C hydrogen bonds from pyridyl protons with an H···N distance of 2.67 Å. The free pyridyl nitrogen atom does not appear to take part in any hydrogen-bonding interactions (the shortest H···N contact is 2.59 Å but is non-directional with C–H···N = 140°).

If the solvent system used for crystallization is changed to DMF/MeOH/H$_2$O then a different complex is obtained, [Co(L^{Et})$_2$(SCN)$_2$]·H$_2$O (**2**), which adopts a different structure despite being constitutionally very similar. The complex **2** crystallizes in the space group *P*2$_1$/*c* with half of the metal atom in the asymmetric unit along with a complete L^{Et} ligand, a SCN ligand, and one interstitial water molecule. The polymeric complex in **2** is topologically the same as that in **1**, i.e., a (4,4) sheet, although the actual form of the sheet is very different, as is the conformation of the ligand (Fig. 3, cf. Fig. 2). The sheets in **2** appear 'squashed' compared with those in **1** with the dimensions of the rings being 10.4 × 24.9 Å^2 (cf. 17.0 × 23.4 Å^2 for **1**) measuring between the Co atoms.

The conformation of the L^{Et} ligand in **2** appears, at first glance, to be similar to that observed in **1** with the arms adopting a *cis*-geometry about the bridging group. However, the ligand

in **2** contains no crystallographic symmetry because of opposing orientations of the pyridyl groups (Fig. 3b). In the structure of L^{Et} the pyridyl nitrogen atoms are on the opposite side of the arm to the pyrazolyl nitrogen atoms, and in the structure of **1** the opposite situation exists. In **2** the L^{Et} ligand adopts a mixture of these two scenarios. The arms are also significantly more twisted than in the preceding two structures with pyridyl/pyrazolyl rotations of 36.5° and 18.4°. The distortion of the (4,4) sheet compared with **1** is so great that there are π-interactions between pyridyl groups within each layer with a CH···centroid distance of 3.37 Å at the narrowest part of each ring (this is directly between the closest pair of Co atoms in the ring). As with the packing of **1** there are also face-to-face π-interactions between neighbouring 2D sheets despite the ligands being significantly deviated from parallel because of the pyrazolyl/pyridyl twisting in the arms. The enclathrated water exists in small cavities within the structure at less than unit occupancy. There does not appear to be any significant intermolecular contacts (it is not near any potential hydrogen-bond acceptor sites) although hydrogen positions could not be experimentally determined.

A third Co(SCN)$_2$-based complex was obtained from a DMF solution and is another solvate of [Co(L^{Et})$_2$(SCN)$_2$]. The compound, [Co(L^{Et})$_2$(SCN)$_2$]·2DMF (**3**), forms a 1D coordination polymer with two L^{Et} ligands bridging between adjacent Co(SCN)$_2$ sites (therefore retaining the same metal/ligand ratio as **1** and **2**). Crystals of **3** form in the space group *P*-1 and contain a complete formula unit in the asymmetric unit. There are two different bridging environments between adjacent metals (each containing only one crystallographically unique L^{Et} ligand), which propagate in an A–B–A–B repeating pattern along the length of the polymeric chain (Fig. 4a). The two bridging environments are quite similar with Co–Co distances of 13.59 and 13.79 Å. Furthermore, the two unique L^{Et} ligands both adopt a similar geometry to that in **2** with the pyridyl/pyrazole nitrogen atoms facing in mixed orientations (see above), although the twisting of the rings within the arms is significantly less (10.6°, 3.9°, 1.1°, and 13.3°). The DMF molecules do not partake in any significant intermolecular interactions and, as observed in the structures of **1** and **2**, the non-bonding pyrazolyl nitrogen atoms are also devoid of supramolecular interactions. Adjacent, parallel chains stack by virtue of edge-to-face CH···π interactions that involve pyridyl rings (H···centroid distance = 2.93 Å) and very weak CH···S interactions (~3 Å). Unlike the packing of the sheets in **1** and **2** there are no face-to-face π-interactions between neighbouring chains in the structure of **3**.

The different structures of the [Co(L^{Et})$_2$(SCN)$_2$] framework in **1**–**3** appears to result from the different solvents that are incorporated into the lattice. The structures of **1** and **2** both contain (4,4) sheets and are conformational supramolecular isomers (using the terminology of Zawarotko and coworkers).[16] The flexibility of the L^{Et} ligand allows for the conformation of the network to change with larger holes present to accommodate the presence of MeCN in **1** and a more collapsed network in **2** in response to the smaller guest molecules. Compound **3** is a structural supramolecular isomer of **1** and **2** as it contains the same chemical components but forms a different network, presumably the result of the larger DMF molecules that are present.

Fe and Zn Complexes

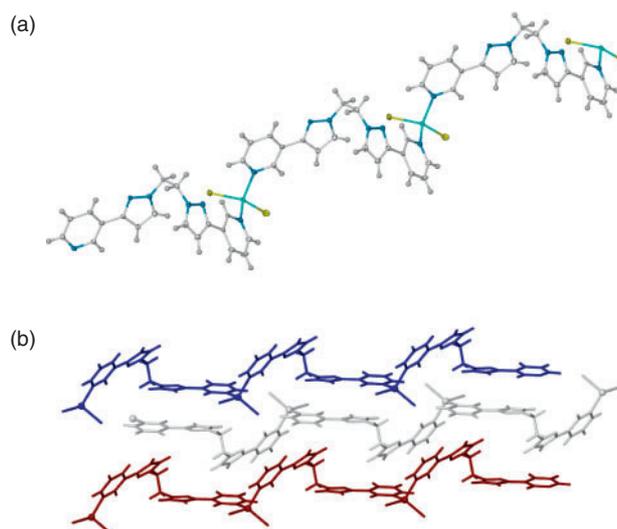In addition to the polymeric complexes **1**–**3**, a discrete complex has also been obtained, [Fe(L^{Et})$_2$(SCN)$_2$(H$_2$O)$_2$] (**4**). The
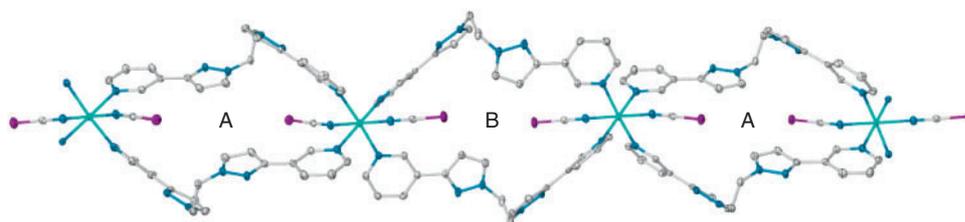
Fig. 4. A portion of the polymeric chain in the structure of $[Co(L^{Et})_2(SCN)_2] \cdot 2DMF$ (**3**) showing the two crystallographically unique bridging environments (A and B). Ellipsoids are displayed at 50% probability, hydrogen atoms and DMF molecules are omitted for clarity.

(a)

(b)

(c)
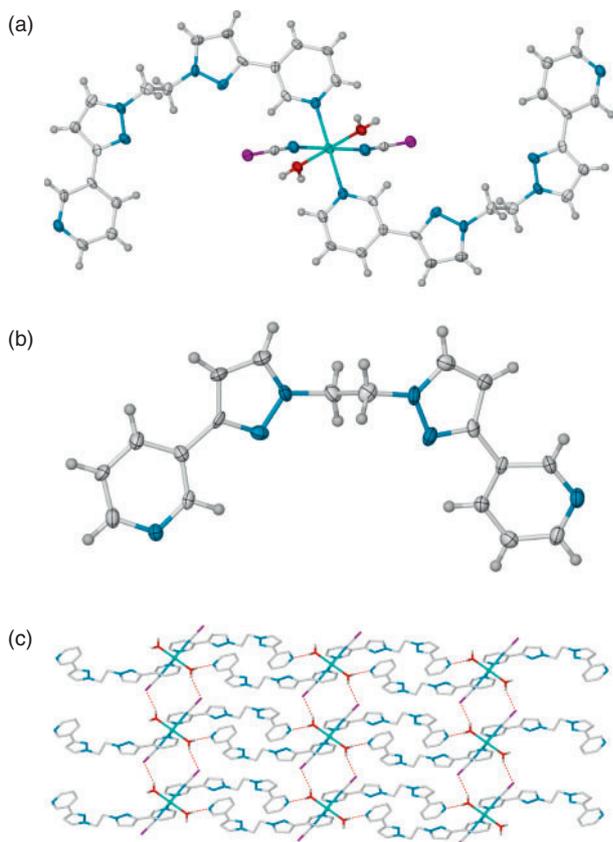
Fig. 5. (a) Structure of the molecular complex $[Fe(L^{Et})_2(SCN)_2(H_2O)_2]$ (**4**) with ellipsoids displayed at 50% probability. (b) The conformation of the L^Et ligand. (c) The discrete complexes pack by $OH\cdots N$ and $OH\cdots S$ interactions to form a hydrogen-bonded sheet (CH hydrogen atoms are omitted for clarity).

(a)

(b)


Fig. 6. (a) A portion of the 1D polymeric chain $[Zn(L^{Et})Cl_2]$ (**5**) and (b) the individual chains pack by face-to-face π-interactions.

centrosymmetric molecular complex contains an octahedral Fe^II with the three types of monodentate ligands located in mutually *trans* positions (Fig. 5a). The metal/L^Et ratio is the same as in the polymeric species **1–3**, however, the presence of coordinated water molecules prevents the formation of a polymeric network in **4**. The L^Et ligand in **4** adopts yet another different conformation from those previously observed. The arms are in a *trans*-geometry about the ethane spacer similar to those in the structure of the free ligand, however, the arms are not coplanar and the ligands adopt a shallow 'u-shaped' conformation (Fig. 5b). The long-range structure of **4** is held together by hydrogen bonds from the aqua ligands to the free pyridyl group and to the sulfur atoms of the thiocyanate anions where $H\cdots X = 1.88$ and 2.51 Å, respectively. These intermolecular interactions lead

to the formation of hydrogen-bonded sheets (Fig. 5c). If the $H\cdots S$ interaction is ignored, then a similarity to the 1D chains in **3** can be noticed with the $Fe-O-H\cdots N$ interaction replacing the $N-Fe$ bond to form the rings within the polymeric chain. There are face-to-face π-interactions between adjacent 2D sheets.

The thiocyanate complexes **1–4** are based around octahedral metals with the L^Et ligands coordinating in mutually *trans*-positions in all cases. To investigate the effect of using a different metal coordination geometry a reaction was carried out with $ZnCl_2$. A crystalline product was obtained with the formula $[Zn(L^{Et})Cl_2]$ (**5**), which has a lower metal/ligand ratio than **1–4** because of the reduced coordination number of the metal, which is tetrahedral. The complex crystallizes in the space group P-1 with a complete formula unit in the asymmetric unit. The L^Et ligand adopts a similar geometry to that seen in the structures of **2** and **3**, with the arms in a *cis*-geometry around the ethane bridge and different orientations of the pyridyl/pyrazolyl nitrogen atoms in the two arms. The bispyridyl ligand bridges between adjacent metals to form a simple 1D chain (Fig. 6).

Conclusions

The L^Et ligand has been demonstrated to be highly flexible and displays a significant variety of bridging distances $(Npy\cdots Npy)$ despite relatively few degrees of freedom (Fig. 7). Rotation around the pyridyl/pyrazolyl bond and the ability to form *trans*/*cis*-geometries around the ethane spacer lead to this geometrical diversity. The separation between the pyridyl nitrogen
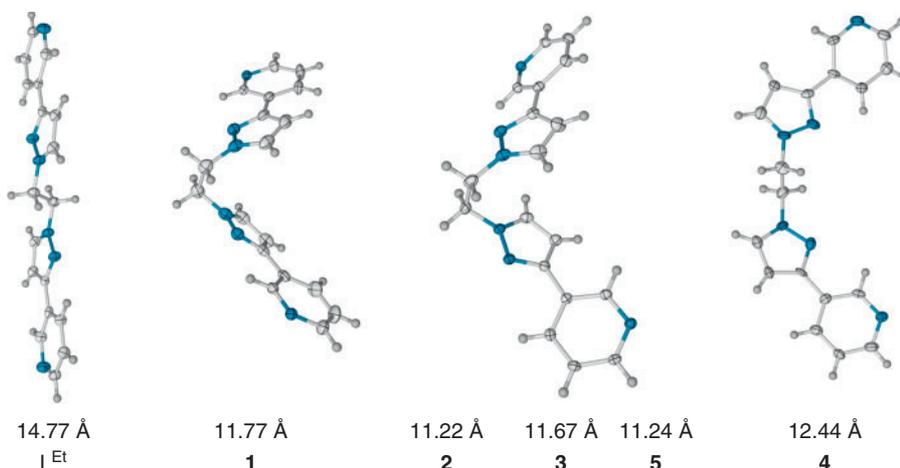
Fig. 7. The different geometries that are adopted by the L^{Et} ligand in the structures reported herein. The N–N distance varies greatly depending on the ligand conformation (distances listed along with the compound numbers in which they occur).

atoms is longest in the structure of the free ligand (14.77 Å), although this geometry is not observed in any of the transition metal complexes. The shortest distances are observed when the arms are arranged in a *cis*-manner around the ethane core in the structures of **1**–**3** and **5**. The length of the terminally coordinated ligand in the structure of **4** is in between these previous situations.

The flexibility of the ligands gives rise to supramolecular isomers of $[Co(L^{Et})_2(SCN)_2]$ in which the coordination framework varies depending on the guest solvent molecules that are present in the crystal lattice.

It is expected that similar ligands with spacers of differing length will also display a variety of geometries, with longer ligands having the potential to form porous or interpenetrating networks, and work towards these ends is ongoing.

Experimental

Synthesis

All reagents were obtained from standard commercial sources and were used without further purification. ^{1}H and ^{13}C NMR spectra were collected using Bruker Avance DRX 200 and DRX 400 spectrometers, respectively. Microanalyses were conducted at the Campbell Analytical Laboratories, University of Otago, New Zealand. IR spectra were recorded as Nujol mulls using a Perkin–Elmer 1600 FT-IR spectrometer. The 3-(3-pyridyl)pyrazole arm (3py3pzH) was synthesized using a literature procedure.[12]

Synthesis of L^{Et}

3py3pzH (5.16 g, 0.0356 mol) was dissolved in toluene (160 mL) and mixed with KOH (65 mL, 5 M), tetrabutyl-ammonium hydroxide (NBu$_4$OH, 0.89 mL, 40% aqueous), and 1,2-dibromoethane (1.53 mL, 0.0177 mol). The mixture was refluxed under N$_2$ for 24 h to form a yellow solution with a fine black precipitate. While the solution was still warm the organic layer was collected. The aqueous layer was washed twice with diethyl ether and the organic layers were combined and dried over anhydrous magnesium sulfate. The organic solution was reduced in volume and stored in a fridge (4°C) for 24 h, which led to the precipitation of a white solid (1.69 g). Further product was obtained by the addition of hexane to the remaining solution

(0.64 g). The product was dried and stored under vacuum over P$_2$O$_5$. Total yield, 2.33 g (42%). δ_H (200 MHz, CDCl$_3$) 9.00 (dd, 1H, *J* 1.33, 0.88), 8.49 (dd, 1H, *J* 3.15, 1.64), 8.13 (ddd, 1H, *J* 3.95, 1.69, 0.59), 7.59 (d, 1H, *J* 2.35), 7.42 (ddd, 1H, *J* 3.92, 2.29, 0.87), 6.75 (d, 1H, *J* 2.33), 4.67 (d, 2H, *J* 4.62). δ_C (100 MHz, CDCl$_3$) 149.53, 148.88, 147.24, 132.83, 132.19, 129.33, 123.63, 103.12, 52.20. (Found: C 67.83, H 4.99, N 26.73. Calc. for C$_{18}$H$_{16}$N$_6$: C 68.34, H 5.10, N 26.56%.) ν_{max}/cm^{-1} 1643w, 1576m, 1462m, 1417s, 1363m, 1290m, 1240s, 1182m, 1122m, 1056s, 1025s, 947s, 924m, 769s, 704s, 619s.

Synthesis of $[Co(L^{Et})_2(SCN)_2]·2MeCN$ (**1**)

A solution of L^{Et} (20 mg, 0.0632 mmol) in DMF/MeCN (1:1, 3 mL) was layered over a solution of CoSO$_4$·7H$_2$O (18 mg, 0.064 mmol) and NaSCN (20 mg, 0.25 mmol) in H$_2$O (3 mL) with a buffer layer of MeCN (2 mL). Pink crystals were formed after a few days at room temperature (14 mg, 52%). (Found: C 56.02, H 4.41, N 24.81. Calc. for C$_{42}$H$_{44}$Co$_1$N$_{16}$S$_2$: C 56.30, H 4.95, N 25.01%.) ν_{max}/cm^{-1} 3107w, 2945w, 2061vs, 1669vs, 1489s, 1387s, 1352s, 1313s, 1090vs, 1052vs, 952s, 815s, 762vs, 730m, 701vs, 658s, 640vs.

Synthesis of $[Co(L^{Et})_2(SCN)_2]·H_2O$ (**2**)

A solution of L^{Et} (20 mg, 0.0632 mmol) in DMF/MeOH (1:1, 3 mL) was layered over a solution of CoSO$_4$·7H$_2$O (18 mg, 0.064 mmol) and NaSCN (20 mg, 0.25 mmol) in H$_2$O (3 mL) with an aqueous buffer layer (2 mL). Pink crystals were formed within a few days at room temperature (16 mg, 61%). (Found: C 56.35, H 4.13, N 24.40. Calc. for C$_{38}$H$_{40}$Co$_1$N$_{14}$S$_2$O$_1$: C 55.27, H 4.15, 23.74%. Calc. for loss of water: C 56.50, H 3.99, N 24.27%.) ν_{max}/cm^{-1} 3101w, 2946w, 2075vs, 1652s, 1607m, 1580m, 1493s, 1421s, 1394s, 1354s, 1304m, 1236s, 1191vs, 1100s, 1074s, 1058s, 1007s, 955s, 810vs.

Synthesis of $[Co(L^{Et})_2(SCN)_2]2DMF$ (**3**)

A solution of L^{Et} (20 mg, 0.063 mmol) in DMF/MeOH (1:1, 3 mL) was layered over a solution of Co(ClO$_4$)$_2$·6H$_2$O (19 mg, 0.052 mmol) and NaSCN (30 mg, 0.38 mmol) in MeCN (3 mL) with a buffer layer of MeCN (3 mL, 0.037 mmol). Pink crystals were formed after leaving the reaction at room temperature for approximately 2 months (21 mg, 70%). (Found: C 55.03, H 4.76, N 23.44. Calc. for C$_{44}$H$_{46}$N$_{16}$O$_2$S$_2$Co$_1$: C 55.39,

H 4.86, N 23.49%.) ν_{max}/cm^{-1} 3107w, 2952w, 2858w, 2081vs, 2058vs, 1669vs, 1607s, 1578m, 1493s, 1425s, 1390s, 1358s, 1316s, 1238vs, 1188s, 1091vs, 1050vs, 953s, 828s, 815s, 760vs, 704vs, 658s, 641vs.

Synthesis of [Fe(L^{Et})$_2$(SCN)$_2$(H$_2$O)$_2$] (4)

A solution of L^{Et} (20 mg, 0.063 mmol) and NaSCN (15 mg, 0.19 mmol) in MeOH (3 mL) was layered over a solution of Fe(ClO$_4$)$_2$·xH$_2$O (16.1 mg, 0.063 mmol) in H$_2$O/EtOH (1:1, 3 mL) with a buffer of H$_2$O/EtOH (1:1, 2 mL). Yellow crystals were formed after approximately 1 month at room temperature (14 mg, 53%). (Found: C 54.27, H 4.37, N 23.32. Calc. for C$_{38}$H$_{36}$Fe$_1$N$_{14}$O$_2$S$_2$: C 54.28, H 4.32, N 23.32%.) ν/cm^{-1} 3403br, 3101w, 2095vs, 1665m, 1604s, 1578s, 1494s, 1466s, 1426vs, 1358s, 1306s, 1235vs, 1193s, 1099s, 1066s, 1052s, 1028vs, 953vs, 924s, 812vs, 787s, 754vs, 731s, 697vs, 640vs, 626s.

Synthesis of [Zn(L^{Et})Cl$_2$] (5)

A solution of L^{Et} (30 mg, 0.095 mmol) in methanol (3 mL) was layered above a solution of ZnCl$_2$ (13 mg, 0.095 mmol) in H$_2$O/EtOH (1:1, 3 mL) with a H$_2$O/EtOH buffer (1:1, 2 mL). Colourless crystals were obtained after approximately 2 months at room temperature (25 mg, 58%). (Found: C 47.76, H 3.63, N 18.32. Calc. for C$_{18}$H$_{16}$Cl$_2$N$_6$Zn$_1$: C 47.76, H 3.56, N 18.57%.) ν/cm^{-1} 3112w, 2944w, 1609m, 1584m, 1493s, 1467s, 1428vs, 1400s, 1355s, 1236vs, 1190s, 1129s, 1097s, 1068s, 1057vs, 957s, 928s, 828s, 814s, 770vs, 747vs, 695vs, 651vs, 636vs.

Crystallography

Single crystals were mounted on fine glass fibres using viscous hydrocarbon oil. Data were collected using either a Bruker X8 Apex II CCD (L^{Et}, 2, 3, and 5) or a Nonius Kappa-CCD (1 and 4) diffractometer, both equipped with monochromated Mo$_{K\alpha}$ radiation ($\lambda = 0.71073$ Å). Data collections were maintained at 123 K using an open-flow N$_2$ cryostream. Data were initially processed using *DENZO*[17] or the *Apex II Program Suite*[18] for the respective instruments. Structures were solved by direct methods using *SHELXS-97*.[19] Refinement was carried out by conventional alternating least-squares cycles against F^2 using *SHELXL-97* and the program X-Seed as a graphical interface.[20] Where possible hydrogen atoms attached to oxygen or nitrogen were experimentally located from the Fourier difference map. Hydrogen atoms attached to carbon were placed in idealized positions and refined using a riding model to the atom to which they were attached. Lp and absorption corrections were applied. Hydrogen atoms of the aqua ligand in 4 were located from the Fourier map and allowed to refine freely while those of the aqua ligand in 2 could not be located from the Fourier map and were not included in the refinement. Crystallographic data (excluding structure factors) for the structures reported in this paper have been deposited with the Cambridge Crystallographic Data Centre as supplementary publication nos. CCDC 707724–707728. Copies of the data can be obtained free of charge on application to the CCDC, 12 Union Road, Cambridge, CB2 1EZ, UK (fax: (+44) 1223 336 033; email: deposit@ccdc.cam.ac.uk).

Crystal Data for L^{Et}

C$_{18}$H$_{16}$N$_6$, M 316.37, colourless block, 0.20 × 0.12 × 0.04 mm^3, monoclinic, space group $P2_1/c$ (No. 14), a 4.8384(9), b 14.737(3), c 10.8477(18) Å, β 90.477(9)°, V 773.5(2) Å^3, Z 2, D_c 1.358 g cm^{-3}, F_{000} 332, $2\theta_{max}$ 49.9°, 2918 reflections collected, 1262 unique (R_{int} 0.0300). Final GoF 1.280, R_1 0.0546,

wR_2 0.1669, R indices based on 1087 reflections with $I > 2\sigma(I)$, 109 parameters, 0 restraints, μ 0.087 mm^{-1}.

Crystal Data for 1

C$_{42}$H$_{44}$Co$_1$N$_{16}$S$_2$, M 895.98, pink block, 0.24 × 0.16 × 0.14 mm^3, orthorhombic, space group *Cmca* (No. 64), a 17.007(3), b 10.855(2), c 23.359(5) Å, V 4312.3(14) Å^3, Z 4, D_c 1.380 g cm^{-3}, F_{000} 1868, $2\theta_{max}$ 55.0°, 15 876 reflections collected, 2524 unique (R_{int} 0.1043). Final GoF 1.058, R_1 0.0557, wR_2 0.1446, R indices based on 1982 reflections with $I > 2\sigma(I)$, 149 parameters, 0 restraints, μ 0.547 mm^{-1}.

Crystal Data for 2

C$_{38}$H$_{34}$Co$_1$N$_{14}$O$_1$S$_2$, M 825.84, pink block, 0.24 × 0.12 × 0.10 mm^3, monoclinic, space group $P2_1/c$ (No. 14), a 9.7528(3), b 10.3760(3), c 19.3784(5) Å, β 100.385(1)°, V 1928.87(10) Å^3, Z 2, D_c 1.422 g cm^{-3}, F_{000} 854, $2\theta_{max}$ 55.0°, 18 983 reflections collected, 4340 unique (R_{int} 0.0350). Final GoF 1.049, R_1 0.0359, wR_2 0.0891, R indices based on 3557 reflections with $I > 2\sigma(I)$, 259 parameters, 0 restraints, μ 0.605 mm^{-1}.

Crystal Data for 3

C$_{44}$H$_{46}$CoN$_{16}$O$_2$S$_2$, M 954.02, pink block, 0.30 × 0.26 × 0.24 mm^3, triclinic, space group P-1 (No. 2), a 9.4422(4), b 13.2078(6), c 20.1759(9) Å, α 71.6960(10)°, β 76.5970(10)°, γ 81.3720(10)°, V 2315.64(18) Å^3, Z 2, D_c 1.368 g cm^{-3}, F_{000} 994, $2\theta_{max}$ 55.0°, 17 696 reflections collected, 10 483 unique (R_{int} 0.0272). Final GoF 1.057, R_1 0.0481, wR_2 0.0945, R indices based on 8715 reflections with $I > 2\sigma(I)$, 599 parameters, 0 restraints, μ 0.517 mm^{-1}.

Crystal Data for 4

C$_{38}$H$_{36}$FeN$_{14}$O$_2$S$_2$, M 840.78, yellow block, 0.16 × 0.10 × 0.10 mm^3, triclinic, space group P-1 (No. 2), a 7.6080(15), b 10.394(2), c 12.723(3) Å, α 90.27(3)°, β 96.73(3)°, γ 100.70(3)°, V 981.4(3) Å^3, Z 1, D_c 1.423 g cm^{-3}, F_{000} 436, $2\theta_{max}$ 50.0°, 8683 reflections collected, 3434 unique (R_{int} 0.1744). Final GoF 0.944, R_1 0.0832, wR_2 0.1698, R indices based on 1400 reflections with $I > 2\sigma(I)$, 268 parameters, 0 restraints, μ 0.545 mm^{-1}.

Crystal Data for 5

C$_{18}$H$_{16}$Cl$_2$N$_6$Zn$_1$, M 452.64, colourless block, 0.16 × 0.16 × 0.14 mm^3, triclinic, space group P-1 (No. 2), a 8.1473(2), b 10.0611(3), c 12.8091(4) Å, α 77.445(2)°, β 74.101(2)°, γ 70.183(2)°, V 940.97(5) Å^3, Z 2, D_c 1.598 g cm^{-3}, F_{000} 460, $2\theta_{max}$ 55.0°, 9990 reflections collected, 4222 unique (R_{int} 0.0387). Final GoF 1.068, R_1 0.0453, wR_2 0.0791, R indices based on 3576 reflections with $I > 2\sigma(I)$, 244 parameters, 0 restraints, μ 1.605 mm^{-1}.

References

[1] J. W. Steed, D. R. Turner, K. J. Wallace, *Core Concepts in Supramolecular Chemistry and Nanochemistry* 2007 (John Wiley and Sons: Chichester).

[2] S. R. Batten, S. M. Neville, D. R. Turner, *Coordination Polymers: Design, Analysis and Application* 2008 (Royal Society of Chemistry: Cambridge).

[3] S. R. Batten, *J. Solid State Chem.* **2005**, *178*, 2475. doi:10.1016/J.JSSC.2005.05.033

[4] G. F. Swiegers, in *Encyclopedia of Supramolecular Chemistry* (Eds J. W. Steed, J. L. Atwood) **2004**, p. 1263 (Marcel Dekker: New York, NY).

[5] (a) R. Robson, *Dalton Trans.* **2008**, 5113. doi:10.1039/B805617J
(b) S. L. James, *Chem. Soc. Rev.* **2003**, 276. doi:10.1039/B200393G

[6] (a) S. R. Batten, *CrystEngComm* **2001**, *3*, 6.7
(b) L. Carlucci, G. Ciani, D. M. Proserpio, *Coord. Chem. Rev.* **2003**, *246*, 247. doi:10.1016/S0010-8545(03)00126-7
(c) J. Bernstein, *Polymorphism in Molecular Crystals* **2002** (Clarendon Press: Oxford).

[7] (a) K. O. Kongshaug, H. Fjellvag, *Inorg. Chem.* **2006**, *45*, 2424. doi:10.1021/IC050662V
(b) D. Min, H. S. Huh, S. W. Lee, *Polyhedron* **2008**, *27*, 2083. doi:10.1016/J.POLY.2008.03.024
(c) G. H. Wang, Z. G. Li, H. Q. Jia, N. H. Hu, J. W. Xu, *Cryst. Growth Des.* **2008**, *8*, 1932. doi:10.1021/CG701232N
(d) D. P. Martin, M. A. Braverman, R. L. LaDuca, *Cryst. Growth Des.* **2007**, *7*, 2609. doi:10.1021/CG700664U
(e) C. J. Wang, H. R. Ma, Y. Y. Wang, P. Liu, L. J. Zhou, Q. Z. Shi, S. M. Peng, *Cryst. Growth Des.* **2007**, *7*, 1811. doi:10.1021/CG070246G
(f) R. Carballo, B. Covelo, M. S. El Fallah, J. Ribas, E. M. Vazquez-Lopez, *Cryst. Growth Des.* **2007**, *7*, 1069. doi:10.1021/CG060616L

[8] (a) L. Carlucci, G. Ciani, S. Maggini, D. N. Proserpio, *CrystEngComm* **2008**, *10*, 1191. doi:10.1039/B803815E
(b) G. C. Xu, Y. J. Ding, T. A. Okamura, Y. Q. Huang, G. X. Liu, W. Y. Sun, N. Ueyama, *CrystEngComm* **2008**, *10*, 1052. doi:10.1039/B803236J
(c) Y. Qi, Y. X. Che, F. Luo, S. R. Batten, Y. Liu, J. M. Zheng, *Cryst. Growth Des.* **2008**, *8*, 1654. doi:10.1021/CG7011217
(d) L. Carlucci, G. Ciani, S. Maggini, D. M. Proserpio, *Cryst. Growth Des.* **2008**, *8*, 162. doi:10.1021/CG700884Q
(e) S. W. Jin, W. Z. Chen, *Polyhedron* **2007**, *26*, 3074. doi:10.1016/J.POLY.2007.02.029
(f) B. X. Dong, J. Peng, C. J. Gomez-Garcia, S. Benmansour, H. Q. Jia, N. H. Hu, *Inorg. Chem.* **2007**, *46*, 5933. doi:10.1021/IC070007I

[9] (a) Z. L. Chu, W. Huang, H. B. Zhu, S. H. Gou, *J. Mol. Struct.* **2008**, *874*, 1. doi:10.1016/J.MOLSTRUC.2007.03.024
(b) Y. Y. Liu, L. Yi, B. Ding, Y. Q. Huang, P. Cheng, *Inorg. Chem. Commun.* **2007**, *10*, 517. doi:10.1016/J.INOCHE.2007.01.013

[10] (a) P. P. Liu, A. L. Cheng, N. Liu, W. W. Sun, E. Q. Gao, *Cryst. Growth Des.* **2008**, *8*, 1668. doi:10.1021/CG701167E
(b) R. Bronisz, *Eur. J. Inorg. Chem.* **2004**, 3688.

[11] (a) S. Ghosh, R. Chakrabarty, P. S. Mukherjee, *Dalton Trans.* **2008**, 1850. doi:10.1039/B713783D
(b) J. Lu, D. R. Turner, S. R. Batten, unpublished results.
(c) C. L. Chen, J. Y. Zhang, C. Y. Su, *Eur. J. Inorg. Chem.* **2007**, 2997. doi:10.1002/EJIC.200700187
(d) X.-Z. Sun, M.-H. Zeng, B. Wang, B.-H. Ye, X.-M. Chen, *J. Mol. Struct.* **2007**, *828*, 10. doi:10.1016/J.MOLSTRUC.2006.05.021

[12] H. Adams, S. R. Batten, G. M. Davies, M. B. Duriska, J. C. Jeffery, P. Jensen, J. Lu, G. R. Motson, S. J. Coles, M. B. Hursthouse, M. D. Ward, *Dalton Trans.* **2005**, 1910. doi:10.1039/B502892B

[13] Y. P. Prananto, D. R. Turner, J. Lu, S. R. Batten, manuscript in preparation.

[14] (a) T. J. Won, J. K. Clegg, L. F. Lindoy, J. C. McMurtrie, *Cryst. Growth Des.* **2007**, *7*, 972. doi:10.1021/CG0700317
(b) V. Mishra, F. Lloret, R. Mukherjee, *Inorg. Chim. Acta* **2006**, *359*, 4053. doi:10.1016/J.ICA.2006.05.005
(c) M. Du, X.-G. Wang, Z.-H. Zhang, L.-F. Tang, X.-J. Zhao, *CrystEngComm* **2006**, *8*, 788. doi:10.1039/B610160G
(d) Q. Cui, X.-Y. Cao, L.-F. Tang, *Polyhedron* **2005**, *24*, 209. doi:10.1016/J.POLY.2004.11.016

[15] (a) K. L. V. Mann, J. C. Jeffery, J. A. McCleverty, M. D. Ward, *J. Chem. Soc., Dalton Trans.* **1998**, 3029. doi:10.1039/A804501A
(b) V. Mishra, F. Lloret, R. Mukherjee, *Inorg. Chim. Acta* **2006**, *359*, 4053. doi:10.1016/J.ICA.2006.05.005
(c) F. Bellouard, M. Clemente-Leon, E. Coronado, J. R. Galan-Mascaros, C. Gimenez-Saiz, C. J. Gomez-Garcia, T. Woike, *Polyhedron* **2001**, *20*, 1615. doi:10.1016/S0277-5387(01)00662-3
(d) C.-S. Liu, X.-S. Shi, *Acta Crystallogr. E* **2007**, *63*, m2139. doi:10.1107/S1600536807032928

[16] (a) T. L. Hennigar, D. C. MacQuarrie, P. Losier, R. D. Rogers, M. J. Zaworotko, *Angew. Chem. Int. Ed. Engl.* **1997**, *36*, 972. doi:10.1002/ANIE.199709721
(b) B. Moulton, M. J. Zaworotko, *Chem. Rev.* **2001**, *101*, 1629. doi:10.1021/CR9900432

[17] Z. Otwinowski, W. Minor, in *Macromolecular Crystallography, Part A. Methods in Enzymology* **1997** (Eds C. W. Carter, Jr, R. M. Sweet) (Academic Press: New York, NY).

[18] Apex2 v2.1-0, Bruker AXS Ltd., Madison (WS), USA.

[19] G. M. Sheldrick, *Acta Crystallogr. A* **2008**, *A64*, 112.

[20] L. J. Barbour, *J. Supramol. Chem.* **2001**, *1*, 189. doi:10.1016/S1472-7862(02)00030-8